Modelling, fabrication and characterization of long period gratings inscribed by femtosecond laser

JOANA VIEIRA[1,2*], TIAGO PAIXÃO[2], PAULO ANTUNES[1,2], MARGARIDA FACÃO[2], ANA M. ROCHA[1]

[1]*Instituto de telecomunicações and University of Aveiro, Campus de Santiago, 3810-193 Aveiro, Portugal*
[2]*i3N & Department of Physics, University of Aveiro, Campus Universitário de Santiago, 3810-193 Aveiro, Portugal*
**joana.saraiva.vieira@av.it.pt*

Abstract: In this paper, we present a method to fabricate long period gratings in standard telecommunications single mode fibers (SSMF), using a femtosecond laser system. A numerical model based on the coupled mode theory was developed and implemented with the aim to guide and improve the inscribing technique. This model takes in consideration the specifications of the inscription technique. Using this model, we have analyzed the behavior of the gratings for different irradiation lengths per period, refractive index modulation values and considering first and second order coupling with different cladding modes. LPGs inscribed in SSMF are presented, its transmission spectra were analyzed and a good agreement between the numerical results and the experimental LPGs was achieved. The sensitivity to temperature of the produced LPGs was also characterized, attaining different sensitivities for different attenuation peaks.

Keywords: long period grating, femtosecond laser, coupled mode theory, refractive index modulation.

1. Introduction

An optical fiber grating corresponds to a periodic modulation of the refractive index of the fiber material. One type of these gratings are the long period gratings (LPGs), whose period is in the range of hundreds of micrometers[1,2]. These gratings are also named transmission gratings and were first proposed by Vengsarkar et al., in 1996 [3]. Light coupling in LPGs occurs between modes travelling in the same direction. In a SSMF this happens among the fundamental core mode and co-propagating cladding modes, resulting in attenuation bands in the transmission spectrum. LPGs can be applied in fiber optical communications [3,4] and as sensors [5–8].

Several methods to fabricate LPGs in optical fibers were already studied. The most common method is the exposition of the optical fiber to radiation, such as, UV laser [9], CO_2 laser [10] or infrared femtosecond laser [11]. These inscription techniques have the advantage of power stability provided by the laser radiation. However, the UV light based inscription requires photosensitive optical fibers, usually highly doped with boron or germanium that are very expensive, when compared with standard telecom fibers, or pretreated with hydrogen loading, that is a time consuming process. The CO_2 laser technique usually presents low reproducibility and high PDL losses, that are a disadvantage for optical communications applications [10,12].

Femtosecond lasers, as the name says, are lasers emitting pulses with a duration of tens or hundreds of 10^{-15} seconds and very high peak energies. Since in light-matter interaction promoted by femtosecond laser pulses the refractive index changes are governed by nonlinear mechanisms, there is no need to use photosensitive optical fibers. Moreover, if a focusing lens is used, the femtosecond laser pulses can be tightly focused within an optical fiber core, modifying only and permanently its refractive index at very well-defined spots. Furthermore, femtosecond laser radiation has shown to be capable of changing the refractive index of various types of glasses [13]. In this way, this method can be used to fabricate LPGs in almost all types of optical fibers, including pure silica core fibers and photonic crystal fibers [14,15]. Kondo et al, in 1999[16] used this method to fabricate LPGs in standard optical fibers for the first time. Since then, the value of refractive index modulation produced by a femtosecond laser that have been reported varies between 10^{-4} and 10^{-2}, negative and positive values [11,14,16–18].

The main goal of the work presented in this paper is to optimize a method for the fabrication of LPGs in standard SMF-28 fibers, using a NIR femtosecond laser and the point-by-point direct writing technique. To guide the fabrication process, a theoretical study of the coupling mechanism of these LPGs was performed. The theoretical

model allowed the variation of different experimental inscribing specifications considering the technique used. Furthermore, the fabricated LPGs sensitivity to temperature was characterized.

2. LPGs fabrication technique

A schematic diagram of the experimental fabrication setup of LPGs by a femtosecond laser is shown in Fig. 1. The used femtosecond laser (model Integra-C 1.0 from Continuum) operates at 800 ± 10 nm with pulses width of 130 fs, a repetition rate of 1 kHz and a maximum pulse energy of 1 mJ. The output laser beam is controlled by a shutter, then rectified by an attenuator, guided by four mirrors (including a dichroic mirror), and focused in the fiber core by a microscope objective lens (PAL50-NIR-HR-LC00 from OptoSigma). The fiber used (SMF-28 from Corning) has a core radius of 4.1 µm, cladding radius of 62.5 µm and NA of 0.14. The position of the optical fiber is controlled by a 3D platform (two MFA-CC from Newport with resolution of 0.1 µm, and one OSMS60-10ZF from OptoSigma with resolution of 0.1 µm). A high-resolution camera was mounted before the microscope objective to assist and monitor the inscription process.

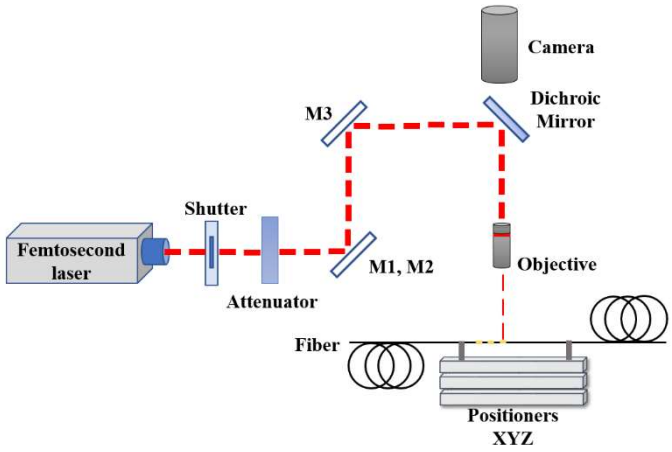

Fig. 1. Schematic representation of the LPGs' fabrication setup. M1-3 are reflective mirrors. For purposes of simplifying the scheme, mirrors M1 and M2 are represented in the same place.

The LPGs were inscribed with the point-by-point direct writing technique. In each point, the NIR femtosecond laser beam was focused on the center of the optical fiber core and the fiber was moved along its length for a distance defined as Lsweep. Next, the femtosecond laser beam was interrupted by closing the shutter and the fiber moved to complete the length defined as the LPG period (Λ). The procedure was repeated until reaching the desired total LPG inscription length, as represented in Fig. 2 a). In Fig. 2 b), a photograph of an inscribed LPG illuminated by a broadband light source is presented, where the inscribed slots are visible due to the scattered light (bright spots). The refractive index modulation (Δn) depends, mainly on the speed with which the optical fiber is moved and the laser optical power. To assure fabrication reproducibility the stability of the system is crucial, so an inscription speed of 0.1 mm/s was used for all LPGs. And to minimize the influence of the positioners' stability, Lsweep values higher than 100 µm could not be used. Furthermore, this fabrication system only allows a maximum inscription length of 25 mm, being this length fixed by the distance between the clamps that hold the optical fiber in the 3D platform.

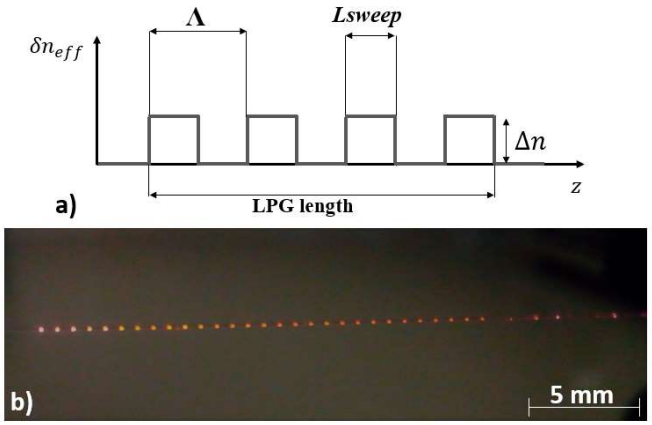

Fig. 2. a) Scheme of the refractive index modulation (Δn), where the period (Λ), Lsweep and LPG length are illustrated. b) Photograph of an LPG inscribed by femtosecond laser radiation, with a Lsweep of 100 μm and a period of 750 μm, illuminated by a broadband light source and showing scattered light (bright spots) at the irradiated sections. The 5 mm marker represents the scale of the image.

3. Theoretical analysis

To simulate the behavior of the LPGs, we used the coupled mode theory [19]. On an ideal waveguide, the propagation modes are orthogonal between them, so no power is coupled. However, in the presence of a grating, that coupling exists and the amplitudes of the modes, A_{j}, in the direction z, are given by:

$$\frac{dA_{\mathrm{j}}}{dz} = i\sum_{\mathrm{k}} A_{\mathrm{k}} K_{\mathrm{kj}}^{\mathrm{t}} \exp\left[i\left(\beta_{\mathrm{k}} - \beta_{\mathrm{j}}\right)z\right]. \tag{1}$$

where β is the propagation constant of the modes. Note that the modes' power is given by $P_j = \left|A_j\right|^2$. The transverse coupling coefficient between the modes j and k is represented by $K_{\mathrm{kj}}^{\mathrm{t}}$, and given by:

$$K_{\mathrm{kj}}^{\mathrm{t}}(z) = \frac{\omega}{4}\iint_{\infty} dxdy\Delta\varepsilon(x,y,z)\boldsymbol{e}_{\mathbf{kt}}(x,y).\boldsymbol{e}_{\mathbf{jt}}{}^{*}(x,y). \tag{2}$$

where ω is the angular frequency, $\Delta\varepsilon$ is the perturbation of the electrical permittivity induced by the grating, $\boldsymbol{e_{kt}}$ and $\boldsymbol{e_{jt}^{*}}$ represent the transversal components of the electrical fields of the propagation modes k and j, where * represents the complex conjugate.

The femtosecond laser technique allows the inscription of gratings only in the core of the fiber due to the ability of focusing the beam inside the core and the absorption being nonlinear. Thus, the superposition integrals are only defined in the core of the fiber, in the form:

$$\sigma_{\mathrm{kj}} = \varepsilon_0 \frac{\omega n_{co}}{2}\overline{\delta n}\iint_{co} dxdy\ \boldsymbol{e}_{\mathbf{kt}}(x,y).\boldsymbol{e}_{\mathbf{jt}}{}^{*}(x,y). \tag{3}$$

In (3), n_{co} represents the refractive index of the core and $\overline{\delta n}$ the maximum value of refractive index modulation. The modulation of the refractive index induced by the femtosecond laser is abrupt. Hence, a sequence of super Gaussians was considered for the modulation form of the refractive index:

$$Y(z) = \sum_{j} \exp\left(-\frac{(z-b_j)^N}{2c^N}\right). \tag{4}$$

where, b_j represents the position of the super Gaussians' maximum, N is the degree of the super Gaussians and $c = \mathrm{FWHM}/2\sqrt[N]{2\ln 2}$ (FWHM is its full-width-half-maximum). This latter quantity can be interpreted as a length in which is made a sweep of laser irradiation on the core of the optical fiber, designated as Lsweep, and shown in Fig. 2 a).

Thus, the transversal coupling coefficient can be rewritten as:

$$K_{\mathrm{kj}}^{\mathrm{t}}(z) = \sigma_{\mathrm{kj}} Y(z). \tag{5}$$

and the equations (1) for the evolution of the modes' amplitude can be rewritten as:

$$\frac{dA_{\mathrm{j}}}{dz} = i\sum_{\mathrm{k}} A_{\mathrm{k}}\,\sigma_{\mathrm{kj}} Y(z)\exp\left[i\left(\beta_{\mathrm{k}} - \beta_{\mathrm{j}}\right)z\right]. \tag{6}$$

Using only two modes, a core mode and a cladding mode and applying the synchronous approximation to equations (6), we obtain an approximation for the LPG period which promote maximum first order coupling given by the implicit equation [19]:

$$\Lambda = \frac{2\pi}{\alpha_0(\Lambda)[\sigma_{11} - \sigma_{22}] + \Delta\beta(\lambda)}. \quad (7)$$

where α_0 is the zero-order term of the Fourier series in which the sequence of super Gaussians can be written. This period is a good approximation for the optimal period in more general conditions.

Moreover, second order coupling LPG periods are given by [20,21]:

$$\Lambda = \frac{4\pi}{\alpha_0(\Lambda)[\sigma_{11} - \sigma_{22}] + \Delta\beta(\lambda)}. \quad (8)$$

3.1 Numerical results

To obtain the electric field distribution ($\boldsymbol{e}$) and the effective refractive indexes (n_{eff}) of the optical modes of the fiber, we used the Wave Optics module of the software COMSOL Multiphysics, assuming a bare fiber surrounded by air. We considered a SSMF with a core of silica doped with GeO_2 (3 %) with a radius of 4.1 μm and a cladding of pure silica with a radius of 62.5 μm. The core and cladding refractive indexes are calculated by the Sellmeier equation [22] that, for a wavelength of 1550 nm, are 1.44853 and 1.44402, respectively.

If the refractive index modulation is azimuthally symmetric, the fundamental core mode ($HE_{1,1}$) will only couple with the cladding modes with the same symmetry, called $HE_{1,m}$ [19]. The effective refractive indexes of the modes considered are in Table 1. Our results are obtained by considering the coupling between two modes, the core fundamental mode and one cladding mode at a time.

Table 1. Effective refractive indexes of the considered modes.

Effective refractive indexes of the modes	
$HE_{1,1}$	1.44574
$HE_{1,2}$	1.44396
$HE_{1,3}$	1.44378
$HE_{1,4}$	1.44347
$HE_{1,5}$	1.44304
$HE_{1,6}$	1.44250
$HE_{1,7}$	1.44184
$HE_{1,8}$	1.44107
$HE_{1,9}$	1.44018
$HE_{1,10}$	1.43919
$HE_{1,11}$	1.43809

The focal point of the femtosecond laser beam used in this work has, approximately, 3 μm of diameter and when the optical fiber core is irradiated only a small volume of the core suffers refractive index modulation. However, we have performed preliminary analysis of the influence of the integration area of the integral (3). We verify that the results obtained with smaller area are equivalent to the results obtained for all the optical fiber core area using a smaller refractive index modulation. Once, from this point forth, all the fiber core area was considered on the simulations and the equivalent refractive index modulation values will be considered.

To understand the behavior of the resonant wavelength for the coupling of the fundamental core mode with different cladding modes, we calculated the resonant wavelength (in the range 1300 nm to 1700 nm), using (7) and (8), for different LPG inscription periods considering Lsweep of 100 μm and different values of refractive index modulation, including positives and negatives values. The results are represented in Fig. 3 for first (full line) and second order coupling (dashed line).

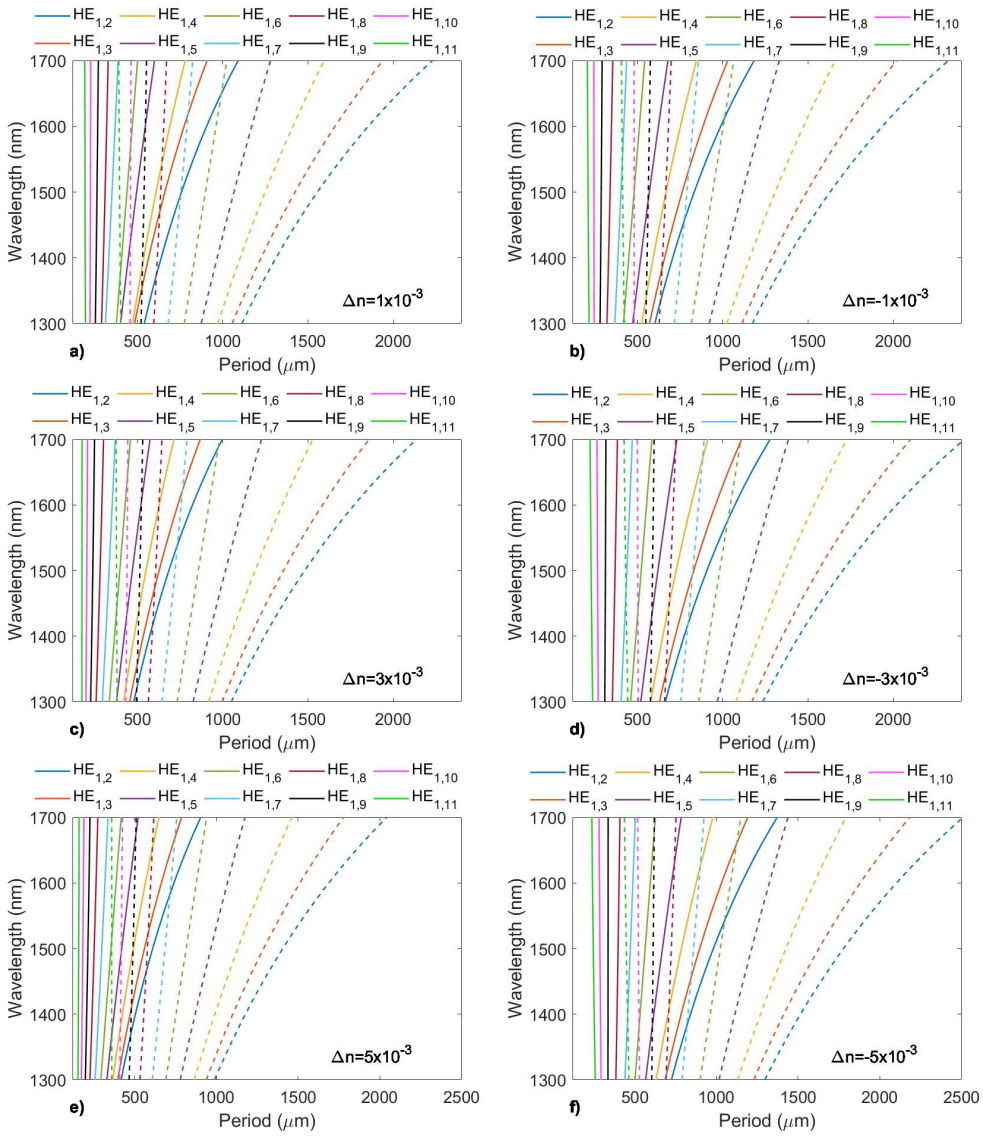

Fig. 3. Dependence of the resonant wavelength with the inscription period for: a) $\Delta n = 1 \times 10^{-3}$, b) $\Delta n = -1 \times 10^{-3}$, c) $\Delta n = 3 \times 10^{-3}$, d) $\Delta n = -3 \times 10^{-3}$, e) $\Delta n = 5 \times 10^{-3}$ and f) $\Delta n = -5 \times 10^{-3}$, for Lsweep of 100 μm. The full and dashed lines represent the results for the first (7) and second (8) coupling order, respectively.

Comparing the results shown in Fig. 3 a), c) and e) for positive values of refractive index modulation, the inscription periods decrease with the increase of the refractive index modulation. On the other hand, for negative values of refractive index modulation on Fig. 3 b), d) and f), the inscription periods increase with the refractive index modulation. Between positive and negative values of refractive index modulation, we observe higher periods for negative ones, and this difference increases with the refractive index modulation. Furthermore, considering the same resonant wavelength, the ideal period decreases for higher modes in all cases. Lastly, when comparing the first with the second order coupling, we verify that, the latter periods are approximately twice as higher than for the first order coupling periods, which reveals that the dependence of α_0 with the period does not contribute very significantly in (7) and (8).

To study the influence of the Lsweep in LPGs, we analyzed the variation of the inscription period and the coupling length, for different Lsweep values and the resonant wavelength of 1550 nm. The coupling length is determined from the full integration of the equations (6), corresponding to the LPG length at which occurs the maximum power coupling between modes. The results are displayed in

Fig. 4. Several values of refractive index modulation, positive and negative, were considered. And, the coupling with different cladding modes were analyzed namely, the coupling of the fundamental core mode $HE_{1,1}$ with the cladding modes $HE_{1,2}$ (a, b, e, f, i and j) and $HE_{1,11}$ (c, d, g, h, k and l), considering the first and second order couplings obtained with (7) and (8), respectively.

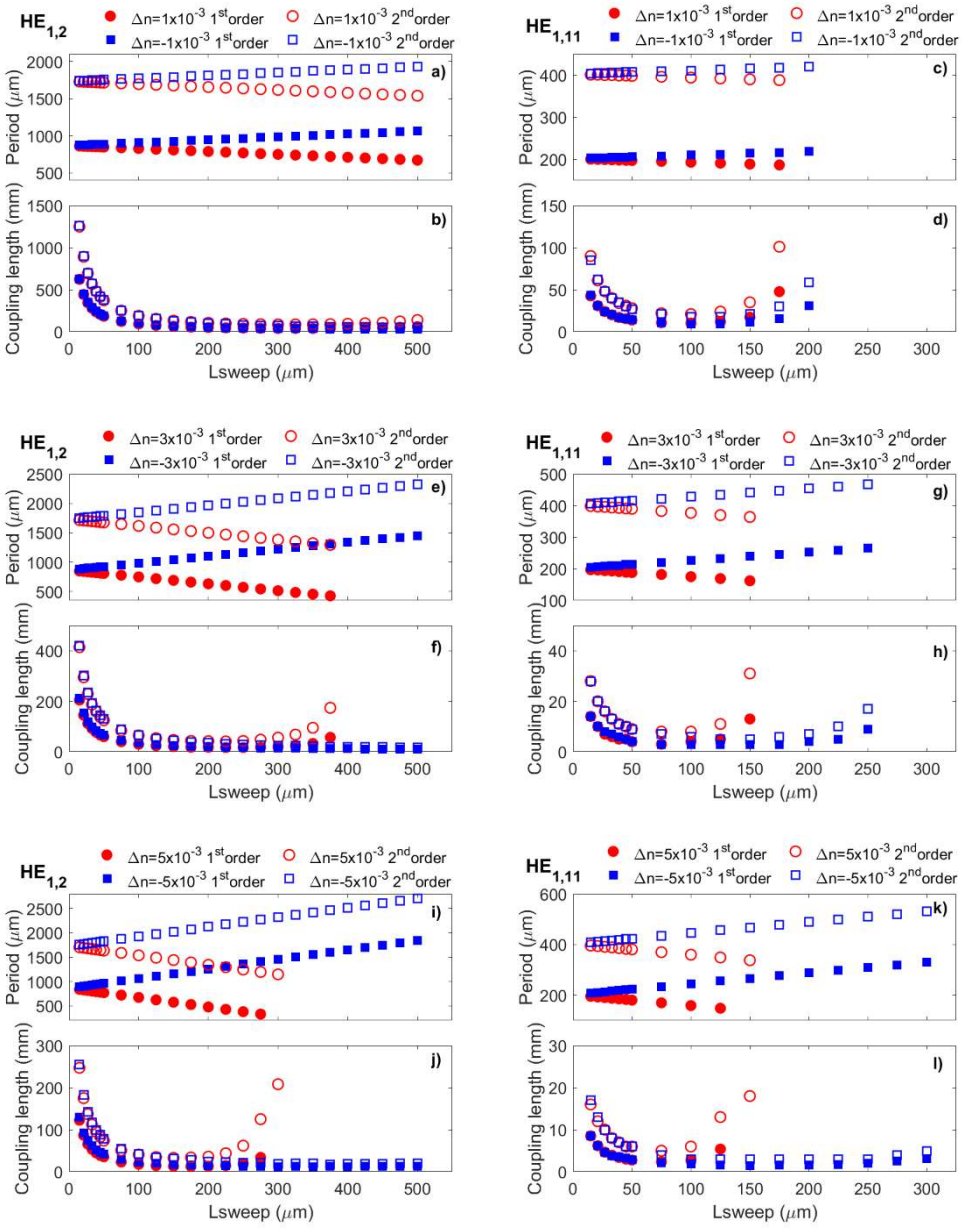

Fig. 4. Variation of the inscription period, (a, c, e, g, i, k), and coupling length, (b, d, f, h, j, l) with Lsweep, considering the first and second order coupling between the modes HE1,1 and HE1,2 and HE1,11, for different values of refractive index modulation and the resonant wavelength of 1550 nm.

Considering the first order coupling, we observe that for positive refractive index modulations, the period decreases in a linear form with Lsweep. This decrease is more pronounced for higher refractive index modulation values. For negative values of refractive index modulation, a symmetric behavior is observed, i.e., the period grows with the same rate as the rate of decrease for the positive ones. The periods obtained when considering the second order coupling have the same behavior described for the first order coupling and are approximately twice as higher.

Regarding the coupling length, the results achieved for first and second order coupling have similar behavior, decreasing rapidly with Lsweep, until values of Lsweep equal half of the period, for all the cases. This decrease is more pronounced for higher refractive index changes. However, the coupling length is always longer for the second

order coupling. Furthermore, for values of Lsweep close to the period, the coupling length increases, being this more pronounced when the second order coupling is considered.

Extending this analysis to the cladding mode $HE_{1,11}$, we can observe that the behavior of both quantities is similar, but the range of periods and coupling lengths are smaller. In fact, for the cladding mode $HE_{1,11}$, the coupling length was found to be one to two orders of magnitude smaller than for the cladding mode $HE_{1,2}$.

4. LPGs fabrication

To fabricate LPGs, we use the technique presented in section 2. Although, the simulations predict that the optimal Lsweep should be equal to half of the period, in order to achieve the lower coupling length possible, Lsweep values higher than 100 µm were not used in order to minimize the influence of the positioners' stability, as mentioned in section 2. The theoretical analysis presented in section 3 indicates that the period should be 700 µm or higher for the coupling with the HE1,2 mode at 1550 nm. Hence, we used these period values as a first approximation.

In this way, two LPGs were fabricated, with periods of 700 and 750 µm and Lsweep of 100 µm, using an average laser power of 350 µW and the maximum inscription length (25 mm). Their transmission spectra were acquired in the wavelength range of 1200 nm to 1700 nm using a broadband light source (Fianium, WL-SC400-2) and an optical spectrum analyzer (OSA) (Advantest, Q8384) and are presented in Fig. 5. Both spectra present several attenuations bands, that correspond to the coupling with different cladding modes.

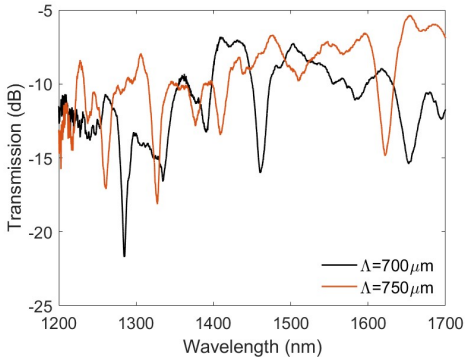

Fig. 5. Transmission spectra of LPGs fabricated with: Lsweep of 100 µm and an average laser power of 350 µW, one with a period of 700 µm, a length of 35 periods and the other one with a period of 750 µm and length of 34 periods.

Using the analysis made in Fig. 3 and comparing with the resonant wavelengths of the attenuation bands of both LPGs from Fig. 5,we found by trial and error, that the refractive index modulation that best fits is $\Delta n = -3 \times 10^{-3}$, for both inscription periods. This comparison is shown in Fig. 6. These results show that the wavelengths of the attenuation bands of the fabricated LPGs are in agreement with the numerical curves, some for first order coupling and others for second order coupling. And, thus, the presented numerical model is adequate for the fabricated LPGs.

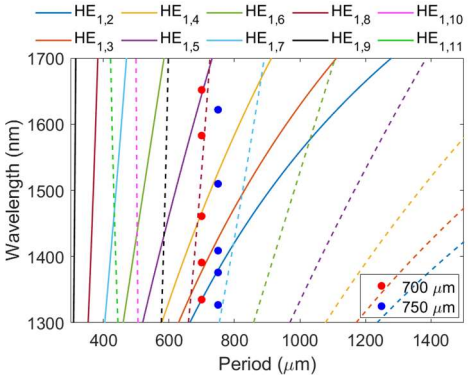

Fig. 6. Comparison between the resonant wavelengths of the attenuation bands of the LPGs fabricated with the calculated resonant wavelength for $\Delta n = -3 \times 10^{-3}$ and Lsweep of 100 µm. The resonant wavelengths of the attenuation bands of the LPG with period of 700 µm are represented by the red dots and the ones for the LPG with period of 750 µm are represented by the blue dots.

4.1 LPGs characterization

To analyze the LPG sensing behavior, we characterized the sensitivity to temperature of two of the attenuation bands (one centered at the wavelength of 1388 nm and the other centered at 1602 nm) of the LPG with period of 750 µm. When a LPG is submitted to different temperatures, a shift in the resonant wavelength of the attenuation band is expected, for different attenuation bands, i.e., different coupling modes, different sensitivities are also expected [8].

In order to perform the thermal characterization, a thermal bath device was used (Lauda, Eco Silver RE 415, resolution of 0.01 ºC) and the LPG response was monitored using the light source and the OSA presented above. The LPG was placed in a Pasteur pipette and sealed with silicone, isolating the LPG from water to prevent interferences in the results due to changes in the environment's refractive index. Then, the pipette with the LPG was submerged in the thermal bath. The thermal characterization was performed by varying the temperature from 25 ºC to 60 ºC, in steps of 5 ºC. A schematic diagram of this experimental setup can be observed in Fig. 7.

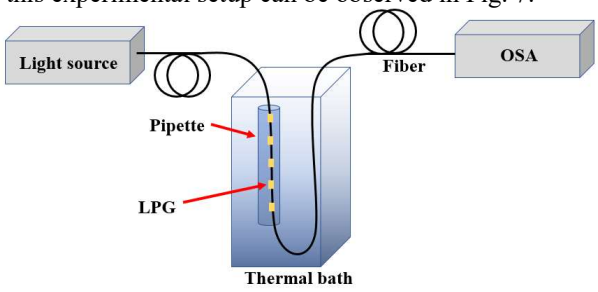

Fig. 7. Schematic diagram of experimental setup for the characterization of the sensitivity of the LPG to temperature.

The results obtained for the dip wavelength shifts with temperature, for the two different attenuation bands, are displayed in Fig. 8. On the inset of the a) and b), we observe the changes of the attenuation band during the increase of the temperature (five steps).

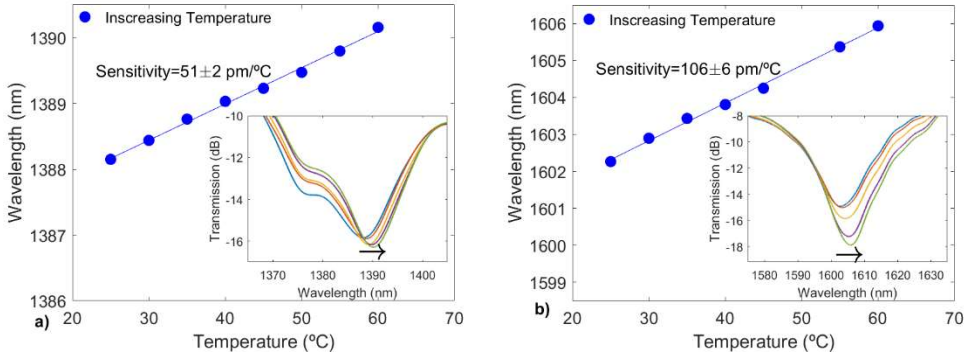

Fig. 8. Dip central wavelength as function of temperature for two attenuation bands centered at the wavelength of 1388 nm (a) and 1602 nm (b), of the LPG with period of 750 µm. The insets display the variation of the attenuation band, during the process of increasing temperature (five steps).

For both attenuation bands, a red shift of the resonant wavelength of the band is observed. When analyzing the theoretical results presented in section 3 namely the wavelength resonances of the Fig. 3 and Fig. 5, and also from prior work [23], it is expected that different attenuation bands have different sensitivities and the higher-order cladding modes have higher sensitivities than lower-order ones. For the attenuation band centered at the wavelength of 1388 nm, that corresponds to a lower-order cladding mode according to Fig. 6, a sensitivity of 51±2 pm/ºC was found. For the attenuation band centered at the wavelength of 1602 nm, a cladding mode of higher order than the one observed before, a sensitivity of 106±6 pm/ºC was found. These results confirm that each attenuation band corresponds to coupling of different modes, the higher-order mode studied has higher sensitivity and the values are also in agreement with the ones studied in the literature [8,16,24].

5. Conclusion

In this paper, the fabrication and characterization of long period gratings inscribed with a femtosecond laser system was studied, theoretically and experimentally. The numerical model allowed the theoretical study of the LPG response for different parameters, such as, the area of integration, refractive index modulation and inscription lengths, guiding the fabrication process. We verified that, for a specific resonant wavelength, the inscription LPG period increases or decreases with the inscription length when the refractive modulation is negative or positive, respectively. The coupling length has a minimum value when the inscription length is, approximately, half of the period. For higher order cladding modes, the range of the periods and coupling lengths are smaller than the ones obtained for the first cladding mode. The dependence of the resonant wavelength with the inscription period was evaluated for coupling with different cladding modes and considering first and second order coupling. The resonant wavelengths of the attenuation bands in the fabricated LPGs show an agreement with the coupling with different cladding modes, for first and second order coupling. A good agreement between the numerical results and the experimental LPGs was achieved and, the numerical model developed allowed to pinpoint an approximation of the refractive index modulation of the fabricated LPGs, being this value of $\Delta n = -3 \times 10^{-3}$. The temperature sensitivity characterization of two different attenuation bands of one of the fabricated LPGs revealed different sensitivities, which confirms that they correspond to the coupling of the core mode with different cladding modes.

Funding: This work was supported by Fundação para a Ciência e Tecnologia (FCT) and by the European Regional Development Fund (FEDER), through the Competitiveness and Internationalization Operational Programme (COMPETE 2020) of the Portugal 2020 framework under the projects MCTechs (POCI-01-0145-FEDER-029282), UIDB/50025/2020 & UIDP/50025/2020, UIDB/50008/2020-UIDP/50008/2020, Tiago Paixão grant PD/BD/128265/2016 and A. M. Rocha contract program 1337.

References

[1] T. Almeida, R. Oliveira, P. André, A. Rocha, M. Facão, R. Nogueira, Automated technique to inscribe reproducible long-period gratings using a CO2 laser splicer, Opt. Lett. 42 (2017) 1994. https://doi.org/10.1364/OL.42.001994.

[2] S.J. Mihailov, C.W. Smelser, D. Grobnic, R.B. Walker, P. Lu, H. Ding, J. Unruh, Bragg Gratings Written in All-SiO2and Ge-Doped Core Fibers with 800-nm Femtosecond Radiation and a Phase Mask, J. Light. Technol. 22 (2004) 94–100. https://doi.org/10.1109/JLT.2003.822169.

[3] A.M. Vengsarkar, P.J. Lemaire, J.B. Judkins, V. Bhatia, T. Erdogan, J.E. Sipe, Long-Period Fiber Gratings as Band-Rejection Filters, J. Light. Technol. 14 (1996) 58–65.

[4] K.S. Chiang, Q. Liu, Long-period grating devices for application in optical communication, 5th Int. Conf. Opt. Commun. Networks,. (2006) 128.

[5] M. Chomát, J. Čtyroký, D. Berková, V. Matějec, J. Kaňka, J. Skokánková, F. Todorov, A. Jančárek, P. Bittner, Temperature sensitivity of long-period gratings inscribed with a CO2 laser in optical fiber with graded-index cladding, Sensors Actuators, B Chem. 119 (2006) 642–650. https://doi.org/10.1016/j.snb.2006.01.013.

[6] J.S. Petrovic, H. Dobb, V.K. Mezentsev, K. Kalli, D.J. Webb, I. Bennion, Sensitivity of LPGs in PCFs Fabricated by an Electric Arc to Temperature , Strain , and External Refractive Index, J. Light. Technol. 25 (2007) 1306–1312.

[7] H. Tsuda, K. Urabe, Characterization of Long-period Grating Refractive Index Sensors and Their Applications, (2009) 4559–4571. https://doi.org/10.3390/s90604559.

[8] W.S. James, P.R. Tatam, Optical fibre long-period grating sensors: characteristics and application, Meas. Sci. Technol. 14 (2003) R49–R61. http://stacks.iop.org/0957-0233/14/i=5/a=201.

[9] V. Bhatia, Properties and Sensing Application of Long-Period Gratings, Faculty of the Virginia Polytechnic Institute and State University, 1996. https://doi.org/10.1007/s004640000247.

[10] D.D. Davis, T.K. Gaylord, E.N. Glytsis, S.G. Kosinski, S.C. Mettler, A.M. Vengsarkar, Long-period fibre grating fabrication with focused CO2 laser pulses, Electron. Lett. 34 (1998) 302–303.

[11] F. Ahmed, H.E. Joe, B.K. Min, M.B.G. Jun, Characterization of refractive index change and fabrication of long period gratings in pure silica fiber by femtosecond laser radiation, Opt. Laser Technol. 74 (2015) 119–124. https://doi.org/10.1016/j.optlastec.2015.05.018.

[12] Y. Wang, Review of long period fiber gratings written by CO2 laser, J. Appl. Phys. 108 (2010) 081101-1-081108–18. https://doi.org/10.1063/1.3493111.

[13] K.M. Davis, K. Miura, N. Sugimoto, K. Hirao, Writing waveguides in glass with a femtosecond laser, Opt. Lett. 21 (1996) 1729–1731.

http://www.jbc.org/.

[14] F. Hindle, E. Fertein, C. Przygodzki, F. Dürr, L. Paccou, R. Bocquet, P. Niay, H.G. Limberger, M. Douay, Inscription of long-period gratings in pure silica and germano-silicate fiber cores by femtosecond laser irradiation, IEEE Photonics Technol. Lett. 16 (2004) 1861–1863. https://doi.org/10.1109/LPT.2004.831264.

[15] S. Liu, L. Jin, W. Jin, D. Wang, C. Liao, Y. Wang, Structural long period gratings made by drilling micro-holes in photonic crystal fibers with a femtosecond infrared laser, Opt. Express. 18 (2010) 5496–5503. https://doi.org/10.1364/oe.18.005496.

[16] Y. Kondo, K. Nouchi, T. Mitsuyu, M. Watanabe, P.G. Kazansky, K. Hirao, Fabrication of long-period fiber gratings by focused irradiation of infrared femtosecond laser pulses, Opt. Lett. 24 (1999) 646–648. https://doi.org/10.1364/ol.24.000646.

[17] E. Fertein, C. Przygodzki, H. Delbarre, A. Hidayat, M. Douay, P. Niay, Refractive-Index Changes of Standard Telecommunication Fiber through Exposure to Femtosecond Laser Pulses at 810 cm., Appl. Opt. 40 (2001) 3506–8. http://www.ncbi.nlm.nih.gov/pubmed/18360376.

[18] J.-M. Savolainen, L. Grüner-Nielsen, P. Kristensen, P. Balling, Determination of femtosecond-laser-induced refractive-index changes in an optical fiber from far-field measurements, Opt. Lett. 39 (2014) 3398. https://doi.org/10.1364/ol.39.003398.

[19] T. Erdogan, Fiber Grating Spectra, J. Light. Technol. 15 (1997) 1277–1294.

[20] P. Fan, L.-P. Sun, Z. Yu, J. Li, C. Wu, B.-O. Guan, Higher-order diffraction of long-period microfiber gratings realized by arc discharge method, Opt. Express. 24 (2016) 25380–25388. https://doi.org/10.1364/oe.24.025380.

[21] J.C. Guo, Y. Sen Yu, X.L. Zhang, C. Chen, R. Yang, C. Wang, R.Z. Yang, Q.D. Chen, H.B. Sun, Compact long-period fiber gratings with resonance at second-order diffraction, IEEE Photonics Technol. Lett. 24 (2012) 1393–1395. https://doi.org/10.1109/LPT.2012.2204243.

[22] Y. Kokubun, Lightwave Engineering, Optical Science and Engineering, Taylor & Francis, 2012. https://doi.org/10.1201/9781315222554.

[23] V. Bhatia, Applications of long-period gratings to single and multi-parameter sensing, Opt. Express. 4 (1999) 457–466.

[24] Y. Zhang, P. Jiang, D. Qiao, Y. Xi, Y. Zhu, Q. Xu, C. Wang, Sensing characteristics of long period grating by writing directly in SMF-28 based on 800 nm femtosecond laser pulses, Opt. Laser Technol. 121 (2020) 105839. https://doi.org/10.1016/j.optlastec.2019.105839.